

Nitride Wide-Bandgap Semiconductors for UV Nonlinear Optics

Subjects: Chemistry, Inorganic & Nuclear

Contributor: Shihang Li, Lei Kang

Nitride wide-bandgap semiconductors possess a wide tunable energy bandgap and abundant coordination anionic groups. This suggests their potential to display nonlinear optical (NLO) properties in the ultraviolet (UV) wavelength spectrum.

Keywords: nitride ; ultraviolet ; nonlinear optical crystal

1. Introduction

Nitrides are significant wide-bandgap semiconductor materials with a variety of optoelectronic applications in different fields of electronic devices, such as high-voltage devices, solar-blind photodetectors, and waveguide devices [1]. Their excellent physical–chemical properties and tunable energy bandgap (E_g) over a wide range make them ideal for these applications. Typical wide-bandgap nitride semiconductors include the third-generation semiconductor GaN [2], ultraviolet (UV) light-emitting material AlN [3] or its solid-solution structure (Ga,Al)N [4], graphene-like layered material h-BN [5], and ceramic material Si₃N₄ [6]. The wide-bandgap E_g rendered the aforementioned materials naturally suitable for use in optoelectronic applications and the study of light–matter interaction in the UV band (100–400 nm). The UV band is typically divided into three segments: UVA (320–400 nm long-wave UV), UVB (280–320 nm mid-wave UV), and UVC (100–280 nm short-wave UV). UVC, in turn, is divided into 200–280 nm solar-blind UV and 100–200 nm deep-UV light [7].

The UV laser is a cutting-edge high-tech solution for UV optoelectronic applications that has added significant value in many areas, including spectroscopy, medicine, and photolithography [8][9][10][11]. One main technical route in UV laser production involves converting traditional micrometer lasers, such as the Nd: YAG 1064 nm laser [12], into UV lasers using the cascade harmonic generation effect of nonlinear optical (NLO) crystals. This typically involves generating 355 nm for the third harmonic generation, 266 nm for the fourth harmonic generation, and 177 nm for sixth harmonic generation based on the fundamental wavelength of 1064 nm [13]. NLO crystals serve as the irreplaceable functional material basis for laser generation, especially for the two crucial solar-blind UV and deep-UV bands. However, the need for NLO performance has increased as second-harmonic-generation (SHG) wavelengths shift to short-wave UV light, posing a challenge in crystal selection [14].

2. Nitride Wide-Bandgap Semiconductors for UV Nonlinear Optics

Note that nitrogen (N) is only less electronegative than fluorine (F) and oxygen (O), similar to chlorine (Cl). Therefore, the relatively weak coupling strength of covalent nitride bonds may lead to a small gap developing between the highest occupied molecular orbitals (HOMO) and the lowest unoccupied molecular orbitals (LUMO). In other words, the energy bandgaps (E_g) of nitrides are typically slightly lower than those of fluorides or oxides. However, nitrides can also be bonded by the continued oxidation of F or O, resulting in the potential creation of fluoronitrides or oxynitrides. These fluoronitride or oxynitride compounds can further increase the energy bandgap E_g , making them appropriate for wider optical transparency at shorter UV wavelengths. It should be emphasized that the NLO effects and birefringence are frequently linked with covalent anionic motifs.

2.1. GaN and AlN with Tetrahedral [GaN₄] or [AlN₄] Motif

Group IIIA nitrides are vital semiconductor materials and they have become the most valuable semiconductor alloy system for short-wavelength light-emitting diodes (LEDs) and laser development, with various applications. The synthesis of binary and ternary nitrides of group IIIA has been critical in the growth of gas phase chemical vapor deposition (CVD) techniques [15].

GaN is a third-generation semiconductor with a wide bandgap $E_g \sim 3.5$ eV [16]. However, its tetrahedral $[\text{GaN}_4]$ framework structure (see **Figure 1a**) results in relatively low structural anisotropy and a small birefringence Δn of only 0.017. Therefore, it cannot meet the requirements for conventional birefringent phase matching in the UV region. AlN, which has the same structure, faces a similar problem. Despite its large bandgap E_g of 6.2 eV [16], the value of birefringence Δn is still small, being only ~ 0.023 , and the material does not have sufficient ability for birefringent phase matching in the UV region. Although it is feasible to develop GaAlN solid solutions with a tunable bandgap E_g , birefringent properties are linked to the local structural anisotropy with minimal improvement. Consequently, such solid solutions remain largely incapable of producing a coherent phase-matching SHG output, especially in the UVC band. This scenario can be observed in $\alpha\text{-Si}_3\text{N}_4$ with the tetrahedral $[\text{SiN}_4]$ motif (see **Figure 1b**).

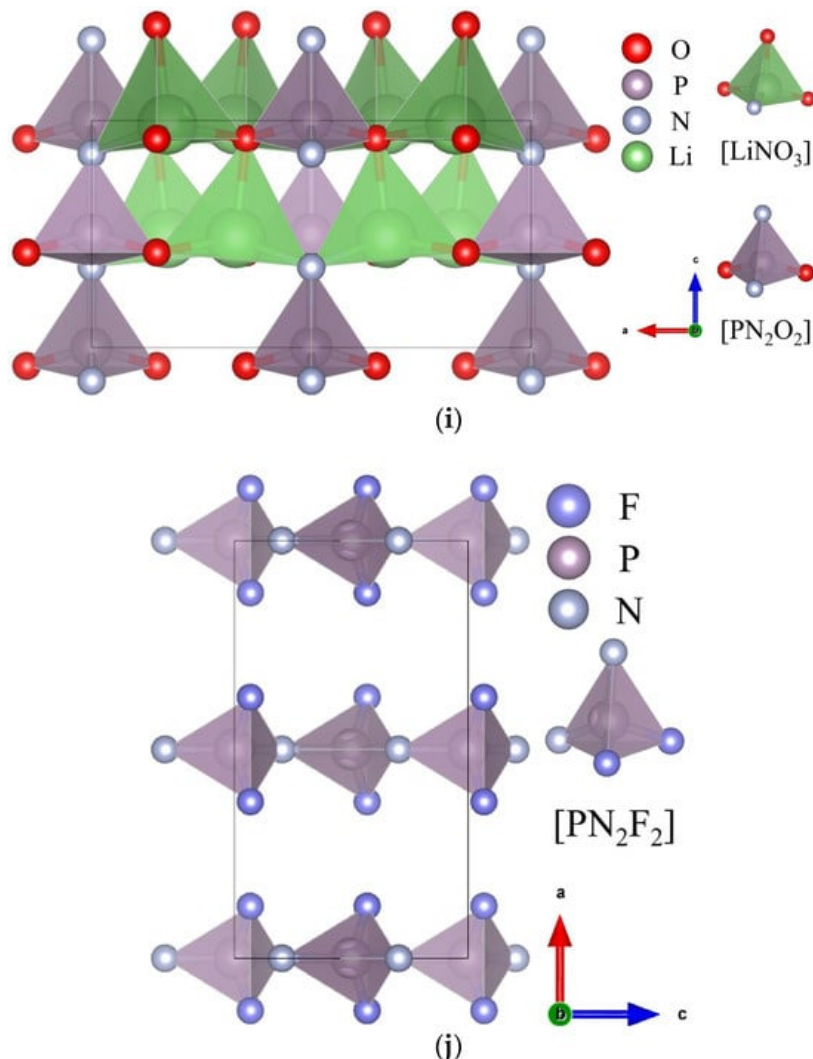


Figure 1. Crystal and motif structures of GaN or AlN (a), Si_3N_4 (b), $\alpha\text{-KCN}$ (c), $\beta\text{-KCN}$ (d), AsC_3N_3 (e), CNi (f), NaCNO (g), $\text{Si}_2\text{N}_2\text{O}$ (h), Li_2PNO_2 (i), and PNF_2 (j). In the legends, a, b, and c indicate the orientation of the crystal axis.

2.2. KCN and AsC_3N_3 with Chained [CN] Motif

An effective scheme to increase the birefringence Δn is to increase the structural anisotropy of the anionic motif. The chain-like [CN] motif is a potential nitride birefringent anionic motif. In a typical KCN compound [17], the CN triple bond determines the bandgap E_g required to reach deep-UV light ($E_g \sim 7.1$ eV for $\alpha\text{-KCN}$ and 7.6 eV for $\beta\text{-KCN}$). The difference in K coordination slightly raises the bandgap E_g from $\alpha\text{-KCN}$ with four coordinations (see **Figure 1c**) to $\beta\text{-KCN}$ with six coordinations (see **Figure 1d**). Despite the staggered arrangement of isolated [CN] motifs, the resulting SHG effects ($d_{15} = 0.76$ pm/V for $\alpha\text{-KCN}$ and $d_{11} = 0.59$ pm/V for $\beta\text{-KCN}$) still exceed those of KDP ($d_{36} = 0.39$ pm/V). Most importantly, their birefringence Δn are both sufficiently large, standing at ~ 0.117 and 0.121, respectively, for $\alpha\text{-KCN}$ and $\beta\text{-KCN}$. Consequently, the $\alpha\text{-KCN}$ and $\beta\text{-KCN}$ crystals can achieve phase-matching SHG output wavelengths of 198 nm and 180 nm, which successfully expand into the deep-UV region. Furthermore, when the pyramid $[\text{AsC}_3]$ motifs with lone-paired electrons (see **Figure 1e**) are combined with the chained [CN] motifs, the bandgap E_g in the resulting AsC_3N_3 [17] structure is determined by the As-C bond, reducing it to $E_g \sim 6.0$ eV.

2.3. CNi and NaCNO with Chained [CNI] or [CNO] Motif

The birefringence and SHG effects can be significantly increased through the parallel alignment of the chained [CN] polar motifs. The coordination of isolated [CN] motifs with iodine (I) forms longer chain-like [CNI] dipole molecules (see **Figure 1f**), which belong to this type of parallelly aligned structure [17]. Consequently, these polar molecule crystals exhibit optimal isotropic alignment with a birefringence Δn of 0.7 and an SHG effect of 16 pm/V. Unfortunately, CNi has a bandgap E_g of ~ 5.3 eV, much smaller than those of KCN, limiting its phase-matching SHG output to only 233 nm, which is insufficient for the deep-UV region, but still sufficient for the solar-blind UV region. Similarly, the [CN] motif in NaCNO coordinates with oxygen (O) to form a [CNO] polar anionic chain (see **Figure 1g**) with a large birefringence Δn of 0.3, allowing the phase-matching SHG output to reach 239 nm [17]. This performance is also achievable for the solar-blind UV band and superior to the UV NLO performance of the classical urea NLO crystal. However, the intrinsic dipole moment of the [CNO] motif is canceled by C and O at both ends, resulting in an SHG effect of only 0.66 pm/V, which is still larger than that of KDP.

2.4. α -Si₃N₄ and Si₂N₂O with Tetrahedral [SiN₄] or [SiN₃O] Motif

Another effective way to increase the structural anisotropy of a tetrahedron is by modifying N with O, which alters the difference in bond lengths of regular tetrahedra. For example, transitioning from α -Si₃N₄ to Si₂N₂O, as shown in **Figure 1h**, elevates the local anisotropy of the tetrahedral [SiN₃O] structure, raises the birefringence Δn of Si₂N₂O to 0.08 (exp. ~ 0.11), and produces a phase-matching SHG output of 285 nm [18]. Regrettably, the structural anisotropy of Si₂N₂O is still not sufficiently extended, which, together with the insufficiently large bandgap $E_g \sim 5.0$ eV, results in a phase-matching SHG output that does not reach the UVC region. Additionally, the SHG effect (e.g., $d_{24} = 1.0$ pm/V) is almost doubled compared to α -Si₃N₄.

2.5. Li₂PNO₂ and PNF₂ with Poly-Chained [PN₂O₂] or [PN₂F₂] Motif

Similar to [SiN₄], the [PN₄] motif exhibits a small degree of structural anisotropy; nevertheless, the bandgap E_g of the P-N bond is generally larger than that of the Si-N bond. By applying the strategy to P-N structures, it may be feasible to extend the UV NLO capacity into the solar-blind UV or even the deep-UV regions. The phosphazene system has been demonstrated to undergo reasonable expansion in this regard [19]. In this case, Li₂PNO₂ alters the [PN] with O, forming a tetrahedral [PN₂O₂] poly-chained arrangement (see **Figure 1i**). As a result, the birefringence Δn increases to 0.067, enabling phase-matching SHG output at 264 nm in the solar-blind UV region. If the [PN] is further modified to become [PN₂F₂] and arranged in a chain-parallel van der Waals (vdW) polymer structure (see **Figure 1j**), the resulting birefringence Δn of the PNF₂ structure increases to 0.16. This yields a phase-matching SHG limit of 142 nm, which is shorter than KBBF's 161 nm limit. It is important to emphasize that this meets the requirements for the application of a 150 nm atomic clock [20].

3. Conclusions

In conclusion, according to a first-principles analysis of structure–property correlations, nitride semiconductors with wide tunable energy bandgaps and abundant coordination motifs are predicted to possess potential UV NLO properties. These properties include wide UV transparency, large SHG effects, sufficient birefringence, and short phase-matching SHG output wavelengths. Regarding nitride NLO materials, a research group has previously made notable contributions to the field [17][18][19]. Since then, the exploration of many nitride NLO materials has flourished. As a short summary, benefits of nitride UV NLO material used include a of UV transmittance equivalent to that of oxides; superior NLO effects; increased anisotropy of the one-dimensional structure, resulting in superior phase-matching capacity; structural diversity in coordination with oxygen or halogen elements; the application of synthetic growth conditions to oxygen-free catalogs of ternary compounds, leading to the development of semiconducting properties; and material stability. Preliminary research indicates that wide-bandgap nitride materials exhibit distinct NLO characteristics across the UV to deep-UV range. Significantly, there is enhanced efficiency in the deep-UV region. This compensates for oxides' lack of deep-UV phase-matching capacity and improves overall NLO harmonic output efficiency in the deep-UV region. These advantages, although previously overlooked, make these materials potential alternatives to oxides and ensure they have a noteworthy impact on the study of inorganic NLO materials.

References

1. Hao, Y.; Zhang, J.F.; Zhang, J.C. Nitride wide bandgap semiconductor material and electronic devices. *MRS Bull.* 2018, 43, 69.

2. Roccaforte, F.; Fiorenza, P.; Greco, G.; Lo Nigro, R.; Giannazzo, F.; Iucolano, F.; Saggio, M. Emerging trends in wide band gap semiconductors (SiC and GaN) technology for power devices. *Microelectron. Eng.* 2018, 187–188, 66–77.
3. Liu, X.; Bruch, A.W.; Gong, Z.; Lu, J.; Surya, J.B.; Zhang, L.; Wang, J.; Yan, J.; Tang, H.X. Ultra-high-Q UV microring resonators based on a single-crystalline AlN platform. *Optica* 2018, 5, 1279–1282.
4. Coulon, P.M.; Kusch, G.; Martin, R.W.; Shields, P.A. Deep UV emission from highly ordered AlGaIn/AlN core-shell nanorods. *ACS Appl. Mater. Interfaces* 2018, 10, 33441–33449.
5. Sharma, V.; Kagdada, H.L.; Jha, P.K.; Spiewak, P.; Kurzydowski, K.J. Thermal transport properties of boron nitride based materials: A review. *Renew. Sustain. Energy Rev.* 2020, 120, 109622.
6. Shen, D.; Shao, Y.; Zhu, Y. Bandgap trimming and optical properties of Si₃N₄: Al microbelt phosphors for warm white light-emitting diodes. *CrystEngComm* 2019, 21, 6566–6573.
7. Chen, H.Y.; Liu, K.W.; Hu, L.F.; Al-Ghamdi, A.A.; Fang, X.S. New concept ultraviolet photodetectors. *Mater. Today* 2015, 18, 493–502.
8. Jones-Bey, H. Deep-UV applications await improved nonlinear optics. *Laser Focus World* 1998, 34, 127–134.
9. Togashi, T.; Nabekawa, N.; Sekikawa, T.; Watanabe, S. Generation of milliwatt narrow-bandwidth vacuum ultraviolet radiation by an all-solid-state tunable high-average-power laser system. *Opt. Lett.* 2001, 26, 831–833.
10. Chen, C.; Sasaki, T.; Li, R.; Wu, Y.; Lin, Z.; Mori, Y.; Hu, Z.; Wang, J.; Aka, G.; Yoshimura, M.; et al. *Nonlinear Optical Borate Crystals, Principles and Applications*; Wiley-VCH Press: Weinheim, Germany, 2012.
11. Savage, N. Ultraviolet lasers. *Nat. Photonics* 2007, 1, 83–85.
12. Wang, X.Z.; Yuan, H.Y.; Wang, M.S.; Huang, W.C. Continuous 1052, 1064 nm dual-wavelength Nd:YAG laser. *Opt. Commun.* 2016, 376, 67–71.
13. Zhang, X.; Wang, L.R.; Wang, X.Y.; Wang, G.L.; Zhu, Y.; Chen, C.T. High-power sixth-harmonic generation of an Nd:YAG laser with KBe₂BO₃F₂ prism-coupled devices. *Opt. Commun.* 2012, 285, 4519–4522.
14. Eismann, U.; Scholz, M.; Paasch-Colberg, T.; Stuhler, J. Short, shorter, shortest: Diode lasers in the deep ultraviolet. *Laser Focus World* 2016, 52, 39–44.
15. Kakanakova-Georgieva, A.; Ivanov, I.G.; Suwannaharn, N.; Hsu, C.-W.; Cora, I.; Pécz, B.; Giannazzo, F.; Sangiovanni, D.G.; Gueorguiev, G.K. MOCVD of AlN on epitaxial graphene at extreme temperatures. *CrystEngComm* 2021, 23, 385–390.
16. Zhao, X.; Lin, C.; Tian, H.; Wang, C.; Ye, N.; Luo, M. Nitrides: A promising class of nonlinear optical material candidates. *Mater. Chem. Front.* 2023; advance article.
17. Kang, L.; Liang, F.; Lin, Z.; Liu, F.; Huang, B. Cyano-based materials with giant optical anisotropy and second harmonic-generation effect. *Inorg. Chem.* 2018, 57, 15001–15008.
18. Kang, L.; He, G.; Zhang, X.; Li, J.; Lin, Z.; Huang, B. Alloy engineering of a polar (Si,Ge)₂N₂O system for controllable second harmonic performance. *Inorg. Chem.* 2021, 60, 7381–7388.
19. Kang, L.; Zhang, X.; Liang, F.; Lin, Z.; Huang, B. Poly(difluorophosphazene) as the first deep-ultraviolet nonlinear optical polymer: A first-principles prediction. *Angew. Chem. Int. Ed.* 2019, 58, 10250–10254.
20. Kang, L.; Lin, Z. Deep-ultraviolet nonlinear optical crystals: Concept development and materials discovery. *Light-Sci. Appl.* 2022, 11, 201.